 CMES, vol.20, no.2, pp.99-110, 2007

An Accurate Refinement Scheme for Inverse Heat Source Location Identifications

Leevan Ling[1] **and Tomoya Takeuchi**[2]

Abstract: We aim to identify the unknown source locations in a two-dimensional heat equation from scattered measurements. In [Inverse Problems, 22(4):1289–1305, 2006], we proposed a numerical procedure that identifies the unknown source locations of 2D heat equation solely based on three measurement points. Due to the nonlinearity and complexity of the problem, the quality of the resulting estimations is often poor especially when the number of unknown is large. In this paper, we purpose a linear refinement scheme that takes the outputs of the existing nonlinear algorithm as initial guesses and iteratively improves on the accuracy of the estimations; the convergence of the proposed algorithm with noisy data is proven. The work is concluded by some numerical examples.

Keyword: Heat equation, inverse problem, point source, locations identification, fundamental solution, convergence

1 Introduction

Inverse source identification problems are important in many branches of engineering sciences. For examples, an accurate estimation of a pollution source in a river [El Badia, Ha Duong, and Hamdi (2005)], a determination of magnitude of groundwater pollution sources [Li, Tan, Cheng, and Wang (2006)] are crucial to environmental protection. Other examples can be found in [Ohnaka and Uosaki (1989); Özişik and Orlande (2000)] and the references therein.

In general, a complete recovery of the unknown source is not attainable from practically restricted boundary measurements. The inverse source problem only becomes solvable if certain *a priori* knowledge is assumed. Since the heat conduction process is irreducible in time and the temperature profile becomes rapidly smoother in time, the characteristic of the solution (for instance, the shape of the interior heat flow) may not be affected by the observed data. To the best knowledge of the author, the mathematical analysis and efficient algorithms for inverse heat problems are still very limited. For instance, the inverse heat conduction problems are studied in [Chang, Liu, and Chang (2005); Hon and Wei (2005); Ling and Atluri (2006)]. The uniqueness and conditional stability results for heat source identification problem can be found in [Choulli and Yamamoto (2004); Ling, Yamamoto, Hon, and Takeuchi (2006); Saitoh, Tuan, and Yamamoto (2002)]. Studies on stationary point source problem can be found in the work of [Baratchart, Ben Abda, Ben Hassen, and Leblond (2005); El Badia and Ha Duong (1998); Kang and Lee (2004)]. Some reconstruction schemes can be carried out in [Park and Chung (2002); Wang and Zheng (2000); Yi and Murio (2004)].

For the sake of simplicity, we formulate our problem in $\mathbb{R}^2$ whereas the extension to $\mathbb{R}^3$ is straightforward. We consider the following heat equation in $\mathbb{R}^2$: for $(t,x) \in \mathbb{R}_+ \times \mathbb{R}^2$,

$$\begin{cases} \dfrac{\partial u(t,x)}{\partial t} &= \Delta u(t,x) + \displaystyle\sum_{k=1}^{N_0} c_k \rho(x-a_k), \\ u(0,x) &= 0, \quad x \in \mathbb{R}^2, \\ u(t,x) &\to 0, \text{ as } |x| \to \infty, \quad \text{for all } t > 0. \end{cases} \tag{1}$$

The *inverse source identification problem* we considered here is stated as follows:

[1] Department of Mathematics, Hong Kong Baptist University, Kowloon Tong, Hong Kong.

[2] Graduate School of Mathematical Sciences, University of Tokyo, Tokyo, Japan.

Determine the total number of source points N_0 and the unknown source locations $\{a_k\}_{1\le k\le N_0} \subset \mathbb{R}^2$ in (1) by some observation data

$$u(b_j,t), \quad 1 \le j \le M,$$

where $M > 0$ and $t \in (t_0,t_1)$ with $0 < t_0 < t_1$ are fixed.

In our first work, we analyzed the above problem with some radially symmetric functions $\rho(\cdot)$ in the Schwartz space $\mathscr{S}(\mathbb{R}^2)$ of rapidly decreasing functions that approximated the dirac-delta function. Furthermore, we assumed that the data are noise-free and all strengths are unitary, e.g. $c_k = 1$ for all k in (1). Recently, we analyze the same problem without such approximation. Besides of the number of sources N_0 and their locations a_k, the strength c_k is now considered as unknown. Moreover, the analysis there takes noise into the account. In both articles, we showed that one measurement point is sufficient to identify the number of sources and three measurement points are sufficient to determine all unknown source positions. Below is a brief summary of the methodology.

Firstly, [Ling, Yamamoto, Hon, and Takeuchi (2006)] showed that $M = 3$ measurement points are sufficient to determine all source locations in two-dimension. The uniqueness of the problem is proven. Later, [Ling and Takeuchi (2007)] considered the same problem with noisy data. After recasting the problem as a nonlinear minimization problem, we are able to show that if the regularization parameter α is chosen properly according to the noise level δ, then the numerical procedures will converge to a sequence of moment equations involving all the target unknowns. Such system of nonlinear equations can then be solved by the pole identification algorithm [Kang and Lee (2004); Nara and Ando (2003)] and allow us to identify the number of source N_0 and their strength c_k and corresponding measurement-to-source distances $r_k = \|b-a_k\|$ for each $b \in \{b_j | 1 \le j \le M\}$. In the $\mathbb{R}^2$ plane, three circles with distinct centers which are not colinear have at most one intersection point. We employ the algorithm in [Vakulenko (2004)] in order to locate the N_0 intersections (or source locations). Details can be found in the original articles.

Numerical demonstrations in our previous study suggest that the proposed method in this paper is capable of identifying the unknown source location in 2D based on the information from as few as three measurement points. Due to the nonlinearity and complexity of the method, the accuracy may not be acceptable in certain cases or some false-positive locations will be found. However, our previously proposed nonlinear methods do successfully provide the initial guess and extra information to some efficient linear solvers for accuracy refinement.

In this paper, we again are interested in the case when $\rho(\cdot)$ is the Dirac delta function. For generality, the analysis in this paper is carried out so that it works for both the Dirac delta function and any radially symmetric functions in the Schwartz space $\mathscr{S}(\mathbb{R}^2)$ of rapidly decreasing functions. Henceforth, $B(c,r)$ denotes the circle centered at c with radius r. Moreover, we assume that the noise level of the input data $u(b_j,t)$ are moderate so that the nonlinear algorithm in [Ling and Takeuchi (2007)] can provide:

- An upper estimation N (with $N \ge N_0$) to the total number of the source points N_0.
- A set of N circles $B(a_k^{(0)}, \varepsilon_k^{(0)})$ $k = 1,\ldots,N$– each of these circles contains exactly one source point.

In Section 2, we propose an iterative linear algorithm that gives accurate refinements to the source locations of (1). Its convergence is proven in the same section. In Section 3, some numerical examples are presented. The sensitivity of various parameters are studied. Moreover, studies on the effect of various parameters are given. Conclusion is given in Section 4.

2 Source locations refinement scheme

In this section, a linear refinement scheme is constructed to further improve the accuracy on the estimations of source locations. Prescribed data to our problem are therefore

$$u(t,b) \text{ for } t \in (t_0,t_1) \text{ and } b \in \mathscr{M}.$$

Here, $\mathscr{M}$ is a set of measurement points $\{b_1,\ldots,b_M\}$ with $M \geq 3$.

We aim to determine the unknown source locations numerically from the *a priori* estimation; namely, the estimated locations given by the precalculation in the form of $B(a_k^{(0)},\varepsilon_k^{(0)})$ for $k = 1,\ldots,N$ with N known. Let $\mathscr{B}^{(0)}$ denote the union of all estimations

$$\mathscr{B}^{(0)} = \bigcup_{k=1}^{N} B(a_k^{(0)},\varepsilon_k^{(0)}). \tag{2}$$

We choose a sequence of points

$$\mathscr{Y}_{N,P} = \{y_p : 1 \leq p \leq N\times P\} \subset \bigcup_{k=1}^{N} B(a_k^{(0)},\varepsilon_k^{(0)}), \tag{3}$$

so that P points are uniformly distributed in each $B(a_k^{(0)},\varepsilon_k^{(0)})$ for $k = 1,\ldots,N$. We call the points y_p to be the *trial centers* at which we place the centers of the fundamental solutions. The method of fundamental solution has been successfully applied to many inverse problems; as an example, [Hon and Wei (2005); Jin and Marin (2007); Wei, Hon, and Ling (2007)]

First of all, the solution for the heat equation (1) is given by

$$u(x,t) = \sum_{k=1}^{N} c_k \int_0^t \int_{\mathbb{R}^2} \frac{1}{4\pi\tau} e^{\left(-\frac{|x-z|^2}{4\tau}\right)} \rho(z-a_k)\, dz\, d\tau, \tag{4}$$

in which the location a_k and the strength c_k are unknowns. We define an approximation function u_n for $(t,b) \in (t_0,t_1)\times\mathscr{M}$ by

$$u_n(t,\, b) = \sum_{p=1}^{N\times P} \lambda_p \int_0^t \int_{\mathbb{R}^2} \frac{1}{4\pi\tau} e^{\left(-\frac{|b-z|^2}{4\tau}\right)} \rho(z-y_p)\, dz\, d\tau, \tag{5}$$

where each λ_p is the corresponding numerical source strength to $y_p \in \mathscr{Y}_{N,P}$. If the measurement point $b \in \mathscr{M}$ are not placed in the convex hull of $\{a_k\}_{1\leq k\leq N_0}$, then the approximation function is well defined.

Motivated by the algorithm given in [Ling, Hon, and Yamamoto (2005)] for the stationary problems, we define a set of collocation points on the measurement point at different time level

$$\mathscr{T}_Q \times \mathscr{M} = \big\{(t_i,b_j) \in (t_0,t_1)\times\mathscr{M} \mid 1 \leq i \leq Q,\, 1 \leq j \leq M\big\}, \tag{6}$$

where $\mathscr{T}_Q := \{t_i \in (t_0,t_1), 1 \leq i \leq Q\}$ is the time sampling. Let $t_i \in \mathscr{T}_Q$ be the time samplings that are distributed uniformly on (t_0,t_1). Collocating (5) at the M distinct measurement points for each t_i, $i \in \{1,\cdots,Q\}$, yields

$$u_n(t_i,\, b_j) \tag{7}$$

$$= \sum_{p=1}^{N\times P} \lambda_p \int_0^t \int_{\mathbb{R}^2} \frac{1}{4\pi\tau} e^{\left(-\frac{|b_j-z|^2}{4\tau}\right)} \rho(z-y_p)\, dz\, d\tau$$

$$= u(t_i,b_j), \quad j = 1,\ldots,M. \tag{8}$$

Equation (8) is equivalent to a linear system of the form

$$A(t_i)\,\lambda = G(t_i), \tag{9}$$

where $A(t_i)$ is a $M\times(NP)$ matrix. The jp-th component of the $A(t_i)$ is given by

$$[A(t_i)]_{jp} = \int_0^{t_i} \int_{\mathbb{R}^2} \frac{1}{4\pi\tau} e^{\left(-\frac{|b_j-z|^2}{4\tau}\right)} \rho(z-y_p)\, dz\, d\tau, \tag{10}$$

with

$$\lambda = [\lambda_1,\ldots,\lambda_{NP}]^T$$

and

$$G(t_i) := [u(t_i,b_1),\cdots,u(t_i,b_3)]^T.$$

Combining (9) for $i = 1,2,\ldots,Q$ yields the following $(MQ)\times(NP)$ system

$$\begin{pmatrix} A(t_1) \\ \vdots \\ A(t_Q) \end{pmatrix} \begin{pmatrix} \lambda_1 \\ \vdots \\ \lambda_{NP} \end{pmatrix} = \begin{pmatrix} G(t_1) \\ \vdots \\ G(t_Q) \end{pmatrix} \text{ or } \Phi\lambda = \zeta. \tag{11}$$

For our numerical computations, we seek for a stable solution of (11) by the least squares optimization. Such approach is commonly used

for solving ill-conditioned or singular system; see [Baumeister (1987); Ling and Kansa (2004, 2005); Ling and Hon (2005)] and references within.

After all the unknown coefficients λ_p in (11) for $p \in \{1, \cdots, N \times P\}$ are obtained, we need to transform the solution in each ball back to a single source locations. The k-th approximated source location associated with the ball $B_k = B(a_k^{(0)}, \varepsilon_k^{(0)})$ is given by

$$a_k^{(1)} := \left(\sum_{\{p: y_p \in B_k\}} \lambda_p \right)^{-1} \sum_{\{p: y_p \in B_k\}} \lambda_p y_p, \quad 1 \le k \le N. \tag{12}$$

Moreover, for each $k = 1, \ldots, N$, we define a set of new estimations by circles centering at $a_k^{(1)}$ with radius $\varepsilon_k^{(1)} := \varepsilon_k^{(0)} / \gamma$ for some $\gamma > 1$.

The proposed method hence provides new estimations to the source locations by (12) and new estimated circles $B_k^{(1)} := B(a_k^{(1)}, \varepsilon_k^{(1)})$. The refinement can be made iterative: we use the output $B_k^{(m)} = B(a_k^{(m)}, \varepsilon_k^{(m)})$, $m \in \mathbb{N}$, to get a new approximation $B_k^{(m+1)} = B(a_k^{(m+1)}, \varepsilon_k^{(m+1)})$ and iterate the computation by distributing the new P trial centers in the new circles. We summarize the above methodology by Algorithm 1.

Algorithm 1 Pseudo-code for the *Source Locations Refinement Scheme*.

Input initial guesses with uncertainty in the form of $\mathscr{B}^{(0)} = \bigcup_{k=1}^{N} B(a_k^{(0)}, \varepsilon_k^{(0)})$ for $k = 1, \ldots, N$
Observe MQ measurement data $u(t,b)$ for $(t,b) \in \mathscr{T}_Q \times \mathscr{M}$
Select a shrink parameter $\gamma > 1$
while $a_k^{(m)}$ for $k = 1, \ldots, N$ has not converged **do**
  for $k = 1, \ldots, N$ **do**
    Place P trial centers y_p uniformly in $B_k^{(m)}$ defined by (2) with radius $\{\varepsilon_k^{(m)}\}$ to form the set $\mathscr{Y}_{N,P}$ as defined in (3)
  end for
  Compute the resultant matrix by (11) and solve the matrix system to find the unknown coefficients associated with $\mathscr{Y}_{N,P}$
  for $k = 1, \ldots, N$ **do**
    Compute the numerical source position $a_k^{(m+1)}$ by (12)
  end for
  Update trust radius $\varepsilon_k^{(m+1)} = \varepsilon_k^{(m)} / \gamma$
end while

Theorem 1 (see [Ling and Takeuchi (2007)]) *If $\alpha = \alpha(\delta)$ and $m = m(\delta)$ are chosen so that $h_{m(\delta)}^2 + \delta^2 = O(\alpha(\delta))$ where $h_{m(\delta)} := \max_{2 \le k \le m(\delta)} \|v_k - v_{k-1}\|_{L^2(0,T)}$, then we have*

$$\lim_{\delta \to 0} \sum_{k=1}^{m(\delta)} \widehat{\lambda}_k g(s_k) = \sum_{k=1}^{N} c_k g(r_k), \tag{13}$$

for all $g \in C^\infty(\mathbb{R}^+)$. In particular, if we take $g(r) = r^n$, we have

$$\lim_{\delta \to 0} \sum_{k=1}^{m(\delta)} \widehat{\lambda}_k s_k^n = \sum_{k=1}^{N_0} c_k r_k^n, \tag{14}$$

for all $n \in \mathbb{R}$

Our previous work shows that, by applying some proper choices of the regularization parameter $\alpha = \alpha(\delta)$ and the denseness of the partition (proportional to m) with respect to the given noise level $\delta > 0$, the unknown coefficients $\hat{\lambda}_k$ determined by solving a nonlinear system will lead to a set of moment equations for any real number n. The exact form of the functional can be found in the original article.

All terms in the right-hand side of (14) are either known *a priori* or obtainable by solving some resultant systems. If we focus only on $n \in \mathbb{N}$, this becomes a pole identification problem.

Let $r_k = \|a_k - b\|$ for $1 \le k \le N$ and suppose that

$$\inf_{1 \le j,k \le N, j \ne k} |r_j - r_k| > 2 \sup_{1 \le k \le N} \varepsilon_k,$$

From Theorem 1, if the measurement-to-source distances are well–separated, we can choose the function g in (13) to be the characteristic function χ_{I_k} where $I_k = [r_k - \varepsilon_k, r_k + \varepsilon_k]$ with C^∞ transient. Considering the i-th measurement point and the

j-th source point results in

$$\lim_{\delta\to 0}\sum_{\{p:y_p\in B_j\}}\widehat{\lambda}_p\|y_p-b_i\|^n=c_jr_j^n,$$

for all $n\in\mathbb{R}$, $j=1,\ldots,N$ and $1\le i\le M$ with $M\ge 3$. We are interested in the case when the power $n=2$. We have

$$\begin{aligned}0&=\lim_{\delta\to 0}\sum_{\{p:y_p\in B_j\}}\widehat{\lambda}_p\|y_p-b_i\|^2-c_jr_j^2\\&=\lim_{\delta\to 0}\sum_{\{p:y_p\in B_j\}}\widehat{\lambda}_p\|y_p-b_i\|^2-c_j\|a_j-b_i\|^2\\&=\lim_{\delta\to 0}\left\{\|b_i\|^2\left(\sum_{\{p:y_p\in B_j\}}\widehat{\lambda}_p-c_j\right)\right.\\&\quad-2\left(\sum_{\{p:y_p\in B_j\}}\widehat{\lambda}_pb_i^Ty_p-c_jb_i^Ta_j\right)\\&\quad\left.+\left(\sum_{\{p:y_p\in B_j\}}\widehat{\lambda}_p\|y_p\|^2-c_j\|a_j\|^2\right)\right\}.\end{aligned}\tag{15}$$

By picking $n=0$, we know that

$$\lim_{\delta\to 0}\sum_{\{p:y_p\in B_j\}}\widehat{\lambda}_p=c_j,\tag{16}$$

and the first quantity in (15) vanishes. Consider $M=3$ for simplicity and note that the last quantity in (15) is constant with respect to all b_i. Subtracting consecutive equations in (15) results in

$$\begin{aligned}(b_1-b_2)^T\left(a_j-\lim_{\delta\to 0}\sum_{\{p:y_p\in B_j\}}\widehat{\lambda}_py_p\right)&=0,\\(b_1-b_3)^T\left(a_j-\lim_{\delta\to 0}\sum_{\{p:y_p\in B_j\}}\widehat{\lambda}_py_p\right)&=0,\end{aligned}$$

as $\delta\to 0$. If the measurement points $b_j=(b_{i,1},b_{i,2})^T$ for $i=1,2,3$ are non-colinear, then the following matrix

$$\begin{bmatrix}b_{1,1}-b_{2,1} & b_{1,2}-b_{2,2}\\ b_{1,1}-b_{3,1} & b_{1,2}-b_{3,2}\end{bmatrix}$$

is nonsingular and hence both x- and y-component in

$$\left(c_ja_j-\lim_{\delta\to 0}\sum_{\{p:y_p\in B_j\}}\widehat{\lambda}_py_p\right)$$

must vanish. Combining (16), we obtain (12).

It remains to show that our linear system gives the correct coefficients $\widehat{\lambda}_k$. We define an operator $K_{NP}:\mathbb{R}^{NP}\to L^2(t_0,t_1)$ by

$$K_{NP}(\widehat{\lambda})(t)=\sum_{\{p:y_p\in\mathscr{B}^{(l)}\}}\widehat{\lambda}_{pk}\int_0^t\frac{1}{(4\pi\tau)^{\frac{d}{2}}}e^{\left(-\frac{\|y_p-b\|^2}{4\tau}\right)}d\tau,$$

for $\widehat{\lambda}\in\mathbb{R}^{NP}$. Following the idea in [Ling and Takeuchi (2007)], the coefficient in Theorem 1 is the unique solution of

$$\begin{cases}K_{NP}^*K_{NP}(\widehat{\lambda})-K_{NP}^*u^\delta+\alpha\xi=0,\\ \xi_k=\dfrac{\widehat{\lambda}_k+\xi_k}{\max\{1,|\widehat{\lambda}_k+\xi_k|\}},\quad 1\le k\le NP.\end{cases}\tag{17}$$

To derive a direct collocation method from the nonlinear system, we need to apply two approximations to the above sections. First, the nonlinear system (17) has to be linearized. Next, the Gram matrix in (17) can be approximated by the normal equation of some overdetermined collocation systems.

As the noise level $\delta\to 0$ and for large number of centers NP, we may assume that the parameter $\alpha\to 0$; see [Ling and Takeuchi (2007)] for details. Hence, the nonlinear system (17) for each $b_i\in\mathscr{M}$ can be linearized to obtain

$$K_{NP}^*K_{NP}(\lambda)=K_{NP}^*u^\delta.\tag{18}$$

Let

$$Y_k(\cdot,t)=\int_{t_0}^t\int_{\mathbb{R}^2}\frac{1}{4\pi\tau}e^{\left(-\frac{\|\cdot-z\|^2}{4\tau}\right)}\rho(z-y_k)\,dz\,d\tau,$$

and the kj-th component of K^*K is given by

$$[K_{NP}^*K_{NP}]_{kj}=\int_{t_0}^{t_1}Y_k(b_i,t)Y_j(b_i,t)\,dt,\tag{19}$$

whereas the k-th component of K^*u is given by

$$[K_{NP}^*u]_k=\int_{t_0}^{t_1}Y_k(b_i,t)u(b_i,t)\,dt.\tag{20}$$

Now, we partition the time interval $[t_0,t_1]$ equally by Q points as in (6). If we approximate (19) and

(20) by some numerical integration schemes, then the linear system (18) can be approximated by

$$A_i^T W A_i \lambda = A_i^T W u_i, \tag{21}$$

where A is a $Q \times NP$ matrix with entries

$$[A_i]_{jk} = Y_k(b_i, t_j) \quad 1 \le j \le Q, 1 \le k \le NP,$$

and the components of u are given by

$$[u_i]_j = u(b_i, t_j) \quad 1 \le j \le Q.$$

Here, $W = \mathrm{diag}(w_j)$ is to be determined by the choice of numerical integration scheme. It is well-known that the solution to (21) is equivalent to the least squares solution to

$$W^{1/2} A_i \lambda = W^{1/2} u_i. \tag{22}$$

Although different numerical schemes result in different non-singular square diagonal weight matrices W, the system (22) is equivalent to

$$A_i \lambda = u_i \tag{23}$$

up to some constant factors. The overdetermined system (23) with all $w_j = 1$ is used in our algorithm to obtain unknown coefficients. In fact, system (22) suggests a possible preconditioning scheme to the least squares collocation system (23). Lastly, we augment (23) for $i = 1, \ldots, M$ to obtain the matrix system (11).

3 Numerical Verifications

In this section, we verify the numerical accuracy of the Algorithm 1 by using an example in found Ling, Yamamoto, Hon, and Takeuchi (2006). We focus on the accuracy of source locations for the case that the function ρ is the Dirac function. In this case the solution (4) of the equation (1) is given by

$$\begin{aligned} u(t, x) &= \sum_{k=1}^{N} \int_0^t \frac{1}{4\pi s} e^{\left(-\frac{|x-a_k|^2}{4s}\right)} ds \\ &= \sum_{k=1}^{N} \frac{1}{4\pi} \int_{\frac{|x-a_k|^2}{4t}}^{\infty} s^{-1} e^{-s} ds \\ &=: \sum_{k=1}^{N} \frac{1}{4\pi} Ei\left(\frac{|x-a_k|^2}{4t}\right), \end{aligned}$$

where Ei is the scaled exponential integral function. Thus, the matrix $A(t_i)$ in (10) is given by

$$[A(t_i)]_{jp} = \frac{1}{4\pi} Ei\left(\frac{|b_j - y_p|^2}{4t_i}\right).$$

We numerically recover the exact source locations

$$\{a_k\}_{k=1}^3 = [\,(0.4, 0), (-0.26, 0.13), (-0.36, -0.33)\,],$$

from the measurement data at

$$\begin{aligned} b_1 &= (1/\sqrt{2},\ -1/\sqrt{2}), \\ b_2 &= (-1/\sqrt{2},\ -1/\sqrt{2}), \\ b_3 &= (0,\ 1). \end{aligned}$$

at some sampling times t_ℓ for $1 \le \ell \le Q$ such that $t_\ell \in [T_{\min}, T_{\max}]$ is equally distributed. We assume that all the radius or uncertainty $\varepsilon_k^{(0)}$ to be 10^{-1} of three estimated circles $B(a_k^{(0)}, \varepsilon_k^{(0)})$ for $k = 1, 2, 3$. We consider two different cases:

Example 1 All exact sources are contained in the first estimated circles $B_k^{(0)}$. Centers of the circles $\{a_k^{(0)}\}_{k=1}^3$ are:

$$\begin{aligned} \{a_k^{(0)}\}_{k=1}^3 = \{&a_1 + (1.7\text{e-}3, 1.7\text{e-}3), \\ &a_2 + (5.8\text{e-}4, 5.8\text{e-}4), \\ &a_3 + (9.5\text{e-}5, 9.5\text{e-}5)\} \end{aligned}$$

Example 2 Some sources are outside in the circle $B_k^{(0)}$ for the sake of applicability.

$$\begin{aligned} \{a_k^{(0)}\}_{k=1}^3 = \{&a_1 + (1.5\text{e-}1, 5.5\text{e-}2), \\ &a_2 + (6.0\text{e-}2, 6.0\text{e-}2), \\ &a_3 + (1.0\text{e-}1, 1.0\text{e-}1)\} \end{aligned}$$

In all computations, the convergence of the algorithm is based on the maximum difference of computed locations in consecutive runs; the stopping criteria is set to be 10e-14 through out of this section.

First, we investigate the effect of increasing numbers of trial centers P. The tested values of P ranged from 3 to 100. For each P, the Algorithm 1 provides three set of estimated locations $\{\hat{a}_1, \hat{a}_2, \hat{a}_3\}$ for each test. The locations of the

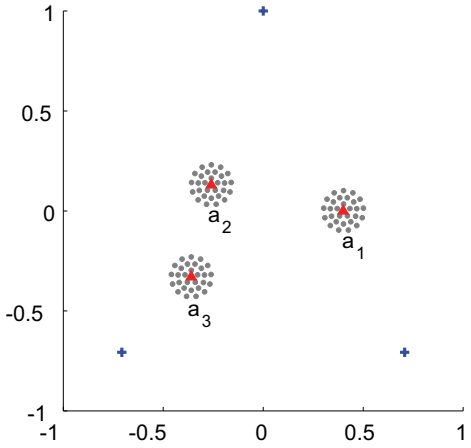

Figure 1: Graphical display of problem setting for Example 1. Three exact source position (▲) and their first estimated circles with $P = 30$ trial centers (•). Three (+) are measurement points.

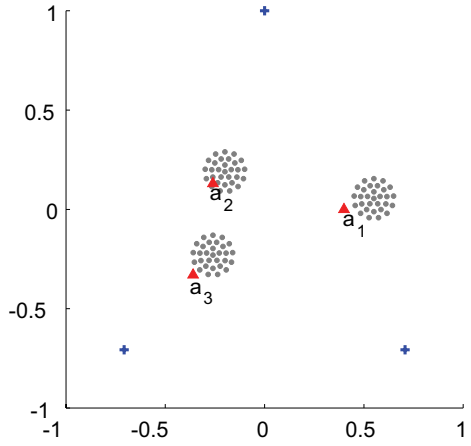

Figure 2: Graphical display of problem setting for Example 2. The source a_1 and a_3 are located outside of their first estimated circles.

source points and the first estimated circle $\mathscr{B}_k^{(0)}$ for $k = 1,2,3$ are showed graphically in Figure 1 and 2.

Figure 3 shows the convergence results of each test for Example 1. In this computation, the number of sampling times is fixed to be $Q = 100$ with various values of $T_{\max} = 5$, 10, 50, and 100. $T_{\min}$ is fixed 10^{-10}. The values of $\max\{|a_1 - \hat{a}_1|, |a_2 - \hat{a}_2|, |a_3 - \hat{a}_3|\}$ are plotted. Algorithm 1 appears to be stable for all tests. The value of $T_{\max}$ has minor influence to the accuracy of the estimated source locations; the maximum errors are stable and accurate with respect to the number of trial centers.

In Example 2, under the same setting, instability appears when $T_{\max} = 5$ and 10. Such instability disappears for large P, see Figure 4.

We continue our analysis on the worst-case. Consider Example 2 when $T_{max} = 5$. In order to see the effect of the parameters P and Q to the accuracy of our algorithm in the case $T_{\max} = 5$ for Example 2, we demonstrate the numerical test with varying P and Q. In Figure 5, the missing dot indicates that the algorithm diverged and the dot indicates the convergence for that particular setting. For each number of time sampling there exists a region for P that the algorithm diverge. But by increasing the number P, we regain the convergence of the algorithm.

Next, we study the effect on increasing numbers of sampling times Q with various values of $T_{\max} =$ 5, 10, 50, and 100. $T_{\min}$ is fixed 10^{-10}, see Figure 6 and 7. The number of trial centers is fixed $P =$ 30. We observe a monotone trend as Q increases and smaller values of $T_{\max}$ show better accuracy.

The heat conduction process is irreducible in time, while the temperature profile becomes rapidly smoother in time. Figure 8 shows the effect of shifting time interval $T = [T_{\min}, T_{\max}]$ for both example. $T_{\min}$ is defined by $T_{\max} - 10$. In this computation the number of sampling times is $Q = 100$ and the numbers of trial centers is $P = 30$. We shift the time interval $T = [T_{\max} - 10, T_{\max}]$ by $T_{\max} = 20, 21, \ldots, 110$. As $T_{\max}$ increases, the accuracy of the algorithm for both cases worsen as expected.

3.1 *Examples with 4 and 6 source points*

Finally, we give the results of the algorithm with 4 and 6 source points:

$$\begin{aligned}\{a_k\}_{k=1}^4 =&[(-0.01,+0.60),\ (+0.43,+0.13),\\ &(-0.26,-0.39),\ (+0.42,-0.54)],\\ \{a_k\}_{k=1}^6 =&[(-0.20,+0.80),\ (+0.70,+0.50),\\ &(-0.20,-0.20),\ (+0.40,-0.30),\\ &(-0.70,-0.50),\ (-0.30,-0.80)].\end{aligned}$$

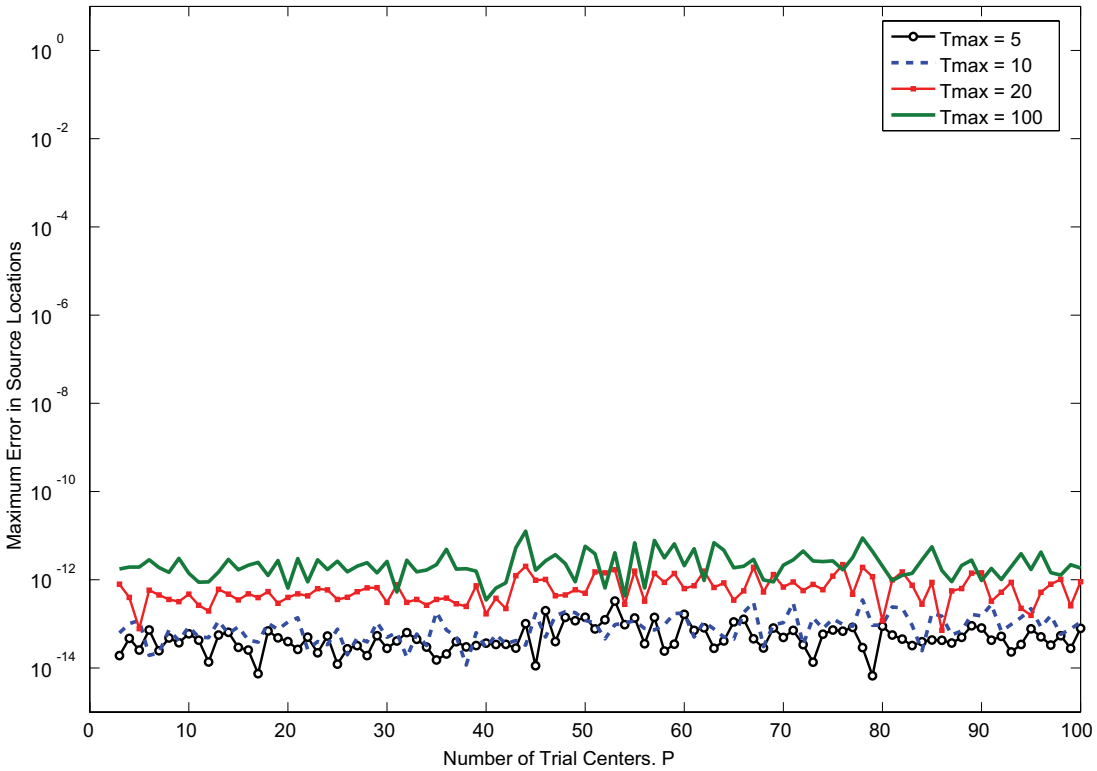

Figure 3: Example 1 with $Q = 100$: The effect of the number of trial centers P to the errors $|a_1 - \hat{a}_1|, |a_2 - \hat{a}_2|$ and $|a_3 - \hat{a}_3|$ where a_k and $\hat{a}_k$ are, respectively the exact and numerical locations.

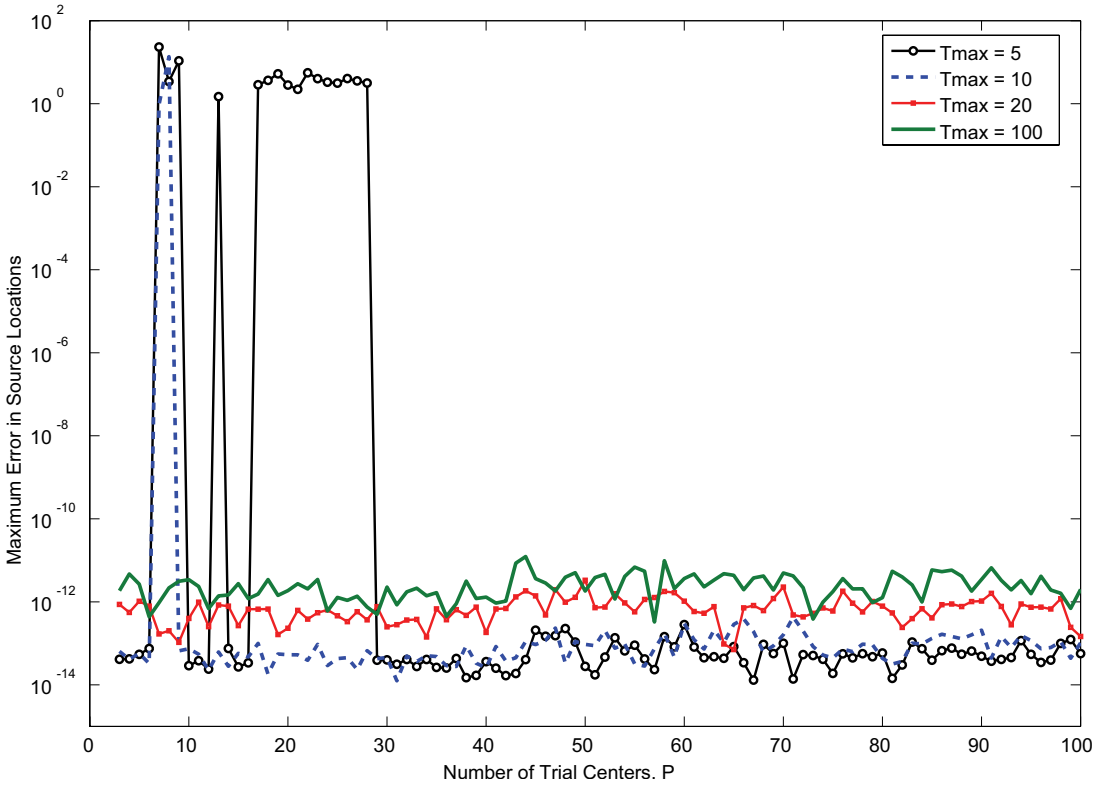

Figure 4: Example 2 with $Q = 100$: The effect of the number of trial centers P to the errors $|a_k - \hat{a}_k|$ for $1 \leq k \leq 3$.

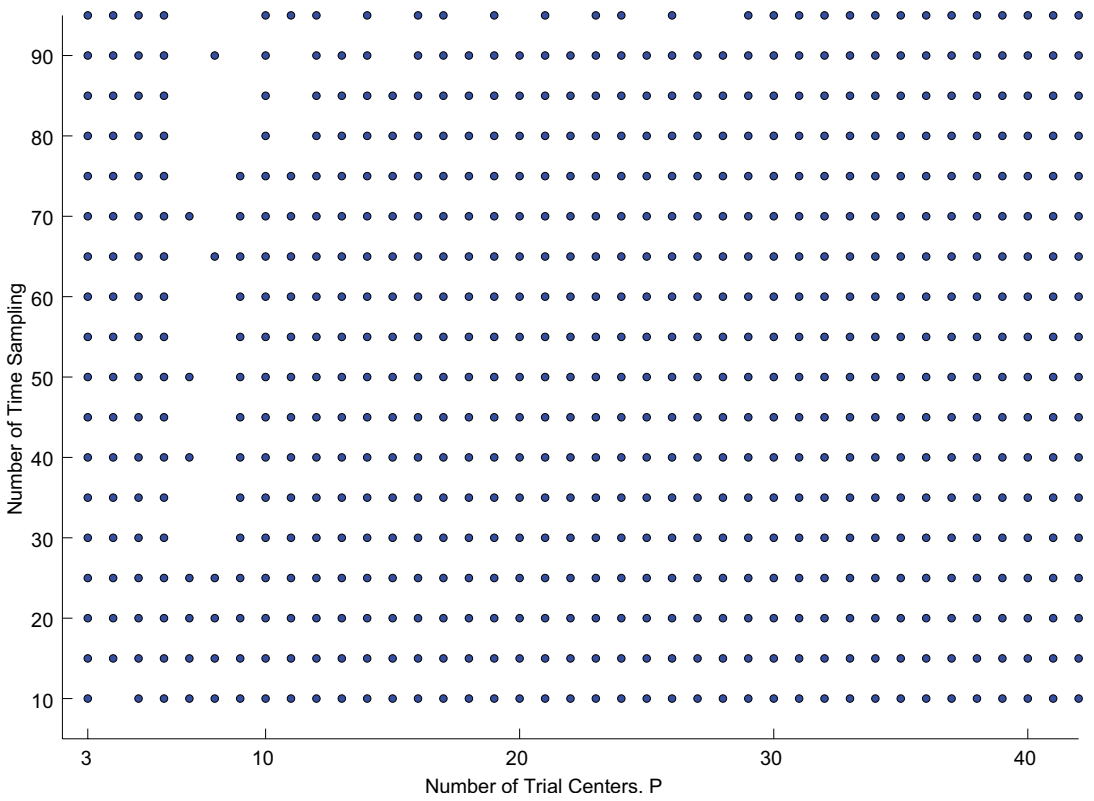

Figure 5: The convergence results for various P and Q for the Example 2. The measurement time interval is fixed to $T = [10^{-10}, 5]$. The dot ($\bullet$) indicates the Algorithm successfully converged to the exact sources. Whereas, the missing dot indicates the Algorithm diverged.

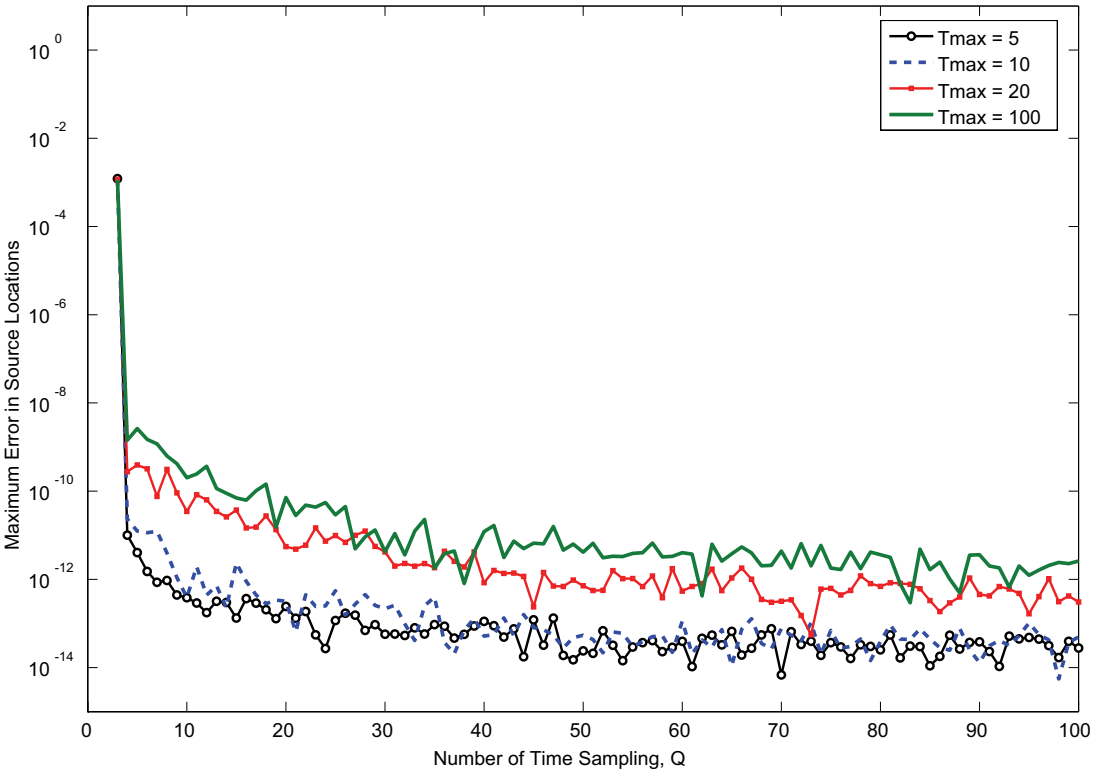

Figure 6: Example 1 with $P = 30$: The effect of the number of time sampling Q to the errors $|a_k - \hat{a}_k|$ for $1 \leq k \leq 3$.

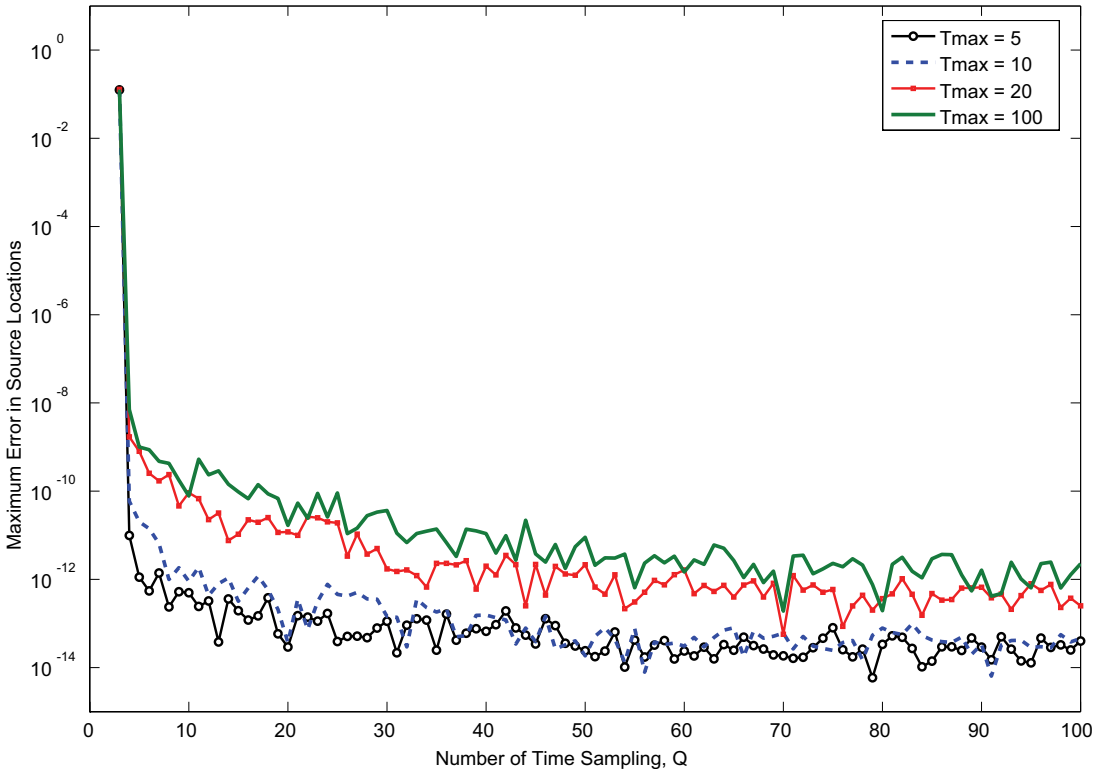

Figure 7: Example 2 with $P = 30$: The effect of the number of time sampling Q to the errors $|a_k - \hat{a}_k|$ for $1 \le k \le 3$.

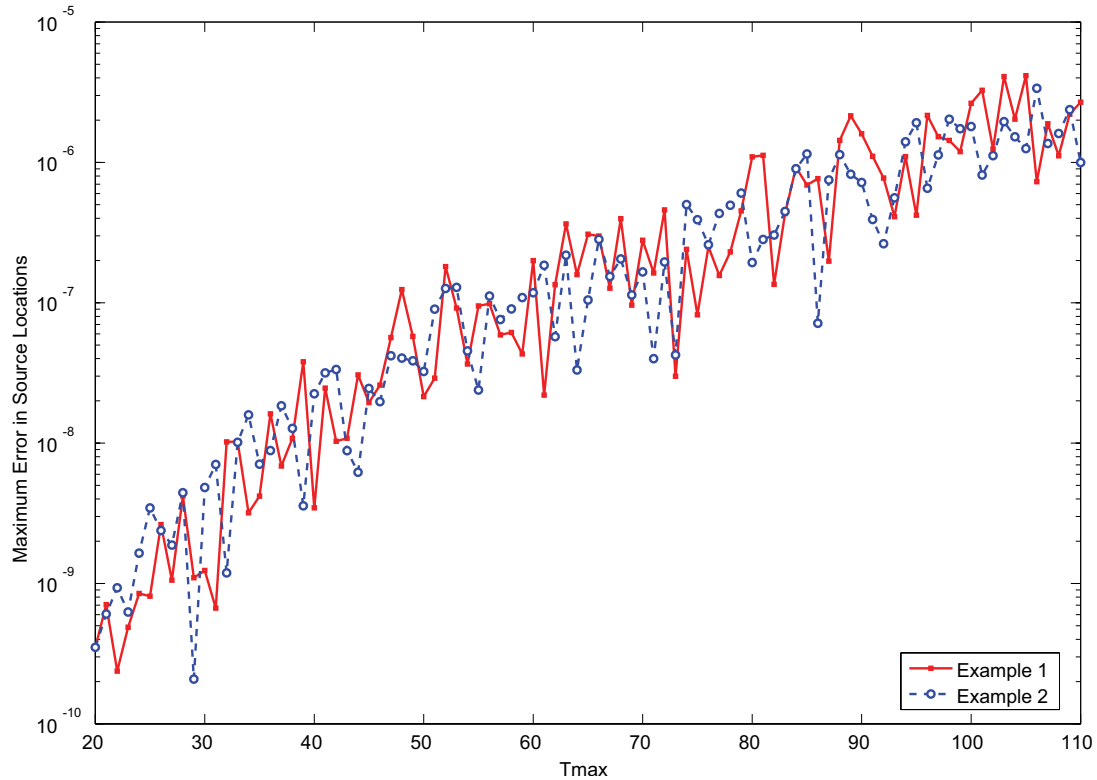

Figure 8: The effect of shifting time interval $T = [T_{\max} - 10, T_{\max}]$ to the errors $|a_k - \hat{a}_k|$ for $1 \le k \le 3$ with $P = 30$ trial centers and $Q = 100$ time sampling. The maximum of the errors is plotted in y-axis.

Table 1: Numerical results for problems with 4 and 6 sources.

	Maximum error	
M	4 sources	6 sources
3	5.4097e-011	3.7582e-004
4	4.3472e-012	1.0331e-008
5	1.2165e-012	6.7345e-010
6	6.1931e-013	5.6379e-011
10	8.3251e-014	9.7918e-012

The centers of the first estimated circles are:

$$\begin{aligned}\{a_k^{(0)}\}_{k=1}^4 =&[(-0.17,+0.55),\ (+0.52,+0.12),\\ &(-0.22,-0.47),\ (+0.49,-0.47)],\\ \{a_k^{(0)}\}_{k=1}^6 =&[(-0.25,+0.90),\ (+0.75,+0.55),\\ &(-0.20,-0.25),\ (+0.45,-0.20),\\ &(-0.65,-.55),\ (-.35,-.85)].\end{aligned}$$

and the radius $\varepsilon_k^{(0)} = 10^{-1}$. The parameters are fixed to be $P = 30$, $Q = 100$, $T = [10^{-10}, 100]$. We test not only the case $M = 3$ measurement points, but also the cases of $M = 4, 5, 6$ and 10. Note that in the cases of $M > 3$, the collocation conditions (8) are merely replaced by $u(t_i,\ b_j) = u_n(t_i,\ b_j)$ for $j = 1, \ldots, M$. Hence the resultant matrix in (11) is of the size $(MQ) \times (NP)$. In each case, M measurement points are uniformly distributed on the unit circle. The maximum errors in source locations are displayed in Table 1. The more information the better–we observe a monotone trend as M increase.

4 Conclusion

We propose a refinement scheme that postprocess the results of a nonlinear source location identification algorithm for the heat equations. Our proposed method successfully refines the approximation to the unknown source locations based on three measurement points. Our work demonstrate that having three measurement points (that is the previously proven minimum requirement for this problem) is also numerically possible to determine all unknown source locations in the inverse heat equation accurately.

We accurately locate all unknowns source locations and source strengths with three examples. Through the given examples, we see that with more than three measurement points it is possible to develop the algorithm that is able to identify more unknown source locations numerically.

Acknowledgements

This work was supported by the FRG Grants (FRG/06-07/II-30) of Hong Kong Baptist University. The second named author was supported partially by the 21 century COE program at the Graduate School of Mathematical Sciences of the University of Tokyo.

References

Baratchart, L.; Ben Abda, A.; Ben Hassen, F.; Leblond, J. (2005): Recovery of pointwise sources or small inclusions in 2D domains and rational approximation. *Inverse Problems*, vol. 21, no. 1, pp. 51–74.

Baumeister, J. (1987): *Stable solution of inverse problems*. Advanced Lectures in Mathematics. Friedr. Vieweg & Sohn, Braunschweig.

Chang, C.-W.; Liu, C.-S.; Chang, J.-R. (2005): A group preserving scheme for inverse heat conduction problems. *CMES: Computer Modeling in Engineering & Science*, vol. 10, no. 1, pp. 13–38.

Choulli, M.; Yamamoto, M. (2004): Conditional stability in determining a heat source. *J. Inverse Ill-Posed Probl.*, vol. 12, no. 3, pp. 233–243.

El Badia, A.; Ha Duong, T. (1998): Some remarks on the problem of source identification from boundary measurements. *Inverse Problems*, vol. 14, no. 4, pp. 883–891.

El Badia, A.; Ha Duong, T.; Hamdi, A. (2005): Identification of a point source in a linear advection-dispersion-reaction equation: application to a pollution source problem. *Inverse Problems*, vol. 21, no. 3, pp. 1121–1136.

Hon, Y. C.; Wei, T. (2005): The method of fundamental solution for solving multidimensional

inverse heat conduction problems. *CMES: Computer Modeling in Engineering & Science*, vol. 7, no. 2, pp. 119–132.

Jin, B. T.; Marin, L. (2007): The method of fundamental solutions for inverse source problems associated with the steady-state heat conduction. *International Journal for Numerical Methods in Engineering*, vol. 69, no. 8, pp. 1570–1589.

Kang, H.; Lee, H. (2004): Identification of simple poles via boundary measurements and an application of EIT. *Inverse Problems*, vol. 20, no. 6, pp. 1853–1863.

Li, G. S.; Tan, Y. J.; Cheng, J.; Wang, X. Q. (2006): Determining magnitude of groundwater pollution sources by data compatibility analysis. *Inverse Probl. Sci. Eng.*, vol. 14, no. 3, pp. 287–300.

Ling, L.; Hon, Y. C. (2005): Improved numerical solver for Kansa's method based on affine space decomposition. *Eng. Anal. Boundary Elements*, vol. 29, no. 12, pp. 1077–1085.

Ling, L.; Hon, Y. C.; Yamamoto, M. (2005): Inverse source identification for Poisson equation. *Inverse Probl. Sci. Eng.*, vol. 13, no. 4, pp. 433–447.

Ling, L.; Kansa, E. J. (2004): Preconditioning for radial basis functions with domain decomposition methods. *Math. Comput. Modelling*, vol. 40, no. 13, pp. 1413–1427.

Ling, L.; Kansa, E. J. (2005): A least-squares preconditioner for radial basis functions collocation methods. *Adv. Comput. Math.*, vol. 23, no. 1-2, pp. 31–54.

Ling, L.; Takeuchi, T. (2007): Point sources identification problem for heat equations. Submitted to *IMA J. Numer. Anal.*, 2007.

Ling, L.; Yamamoto, M.; Hon, Y. C.; Takeuchi, T. (2006): Identification of source locations in two-dimensional heat equations. *Inverse Problems*, vol. 22, no. 4, pp. 1289–1305.

Ling, X.; Atluri, S. N. (2006): Stability analysis for inverse heat conduction problems. *CMES: Computer Modeling in Engineering & Science*, vol. 13, no. 3, pp. 219–228.

Nara, T.; Ando, S. (2003): A projective method for an inverse source problem of the Poisson equation. *Inverse Problems*, vol. 19, no. 2, pp. 355–369.

Ohnaka, K.; Uosaki, K. (1989): Boundary element approach for identification of point forces of distributed parameter systems. *Internat. J. Control*, vol. 49, no. 1, pp. 119–127.

Özişik, M. N.; Orlande, H. R. B. (2000): *Inverse heat transfer: fundamentals and applications*. Hemisphere Pub.

Park, H. M.; Chung, J. S. (2002): A sequential method of solving inverse natural convection problems. *Inverse Problems*, vol. 18, no. 3, pp. 529–546.

Saitoh, S.; Tuan, V. K.; Yamamoto, M. (2002): Reverse convolution inequalities and applications to inverse heat source problems. *JIPAM. J. Inequal. Pure Appl. Math.*, vol. 3, no. 5, pp. Article 80, 11 pp.

Vakulenko, A. (2004): Circles intersection. Technical report, 2004. From *MATLAB Central File Exchange*–File Id: 5313. http://www.mathworks.com/.

Wang, P.; Zheng, K. (2000): Reconstruction of heat sources in heat conduction equations. *Comput. Appl. Math.*, vol. 19, no. 2, pp. 231–238.

Wei, T.; Hon, Y. C.; Ling, L. (2007): Method of fundamental solutions with regularization techniques for cauchy problems of elliptic operators. *Eng. Anal. Boundary Elements*, vol. 31, no. 2, pp. 163–175.

Yi, Z.; Murio, D. A. (2004): Source term identification in 1-D IHCP. *Comput. Math. Appl.*, vol. 47, no. 12, pp. 1921–1933.